

# 中国激光

## 基于荧光光谱法的皮肤胆固醇快速无创检测技术

吴鹏<sup>1,2</sup>, 倪敬书<sup>2,4</sup>, 洪海鸥<sup>3</sup>, 李晓静<sup>3</sup>, 姚蓓<sup>3</sup>, 郑浩然<sup>3</sup>, 花昌义<sup>2,4</sup>, 王霞<sup>2,4</sup>, 张元志<sup>2,4</sup>,  
张洋<sup>2,4</sup>, 王贻坤<sup>2,4</sup>, 董美丽<sup>2,4\*</sup>

<sup>1</sup>安徽师范大学物理与电子信息学院, 安徽 芜湖 241000;

<sup>2</sup>中国科学院合肥物质科学研究院安徽光学精密机械研究所, 安徽省医用光学诊疗技术与装备工程实验室,  
安徽 合肥 230026;

<sup>3</sup>中国科学技术大学附属第一医院健康管理中心, 安徽 合肥 230001;

<sup>4</sup>皖江新兴产业技术发展中心, 安徽省生物医学光学仪器工程技术研究中心, 安徽 铜陵 244000

**摘要** 皮肤胆固醇含量可以作为评价动脉粥样硬化的重要指标之一,现有的皮肤胆固醇含量检测主要基于实验室活检进行,缺少快速无创的检测技术和装备。针对以皮肤胆固醇含量为评价指标的动脉粥样硬化的早期快速筛查需求,本文提出了基于荧光光谱法的皮肤胆固醇快速无创检测方法,研发了一种皮肤胆固醇无创检测系统。为了提高测量的准确性和稳定性,该系统对温度引起的检测试剂荧光效率的波动进行了修正。本文结合气相色谱法对测量结果的准确性进行了验证,并通过检测正常人群和动脉粥样硬化高风险人群的皮肤胆固醇含量,明确了该系统的临床应用价值。本文的研究结果表明,462~520 nm 波段内的平均荧光强度与温度的相关系数为 -0.995 ( $p < 0.0001$ ),可据此建立温度校准曲线对由温度差异引起的荧光波动进行修正。校正后,系统测量的皮肤胆固醇含量与气相色谱测量值的相关性显著,相关系数为 0.905 ( $p < 0.0001$ )。在动脉粥样硬化高风险人群的筛查实验中,动脉粥样硬化高风险人群和正常人群的皮肤胆固醇检测结果具有显著差异 ( $P = 0.0004$ )。与现有技术相比,基于荧光光谱法的皮肤胆固醇检测技术具有测量快速无创等优势,为大规模开展动脉粥样硬化的早期风险筛查提供了先进技术手段。

**关键词** 医用光学; 皮肤胆固醇; 荧光光谱法; 无创检测; 动脉粥样硬化

中图分类号 TN29

文献标志码 A

doi: 10.3788/CJL202148.0307002

### 1 引言

心血管疾病为全球死因之首,且流行趋势不断加剧。动脉粥样硬化是心血管疾病的基础病理,其基本病变为动脉内膜脂质沉积,内膜出现灶状纤维化,粥样斑块形成,导致管壁变硬、管腔狭窄,并引起相应继发性病变。《动脉粥样硬化性疾病的一级预防》中指出,在症状出现前的早期病理阶段有效控制致病因素,可延缓或阻止无症状动脉粥样硬化发展成临床心血管疾病。可见,动脉粥样硬化的早期检

测是心血管疾病防治工作的重中之重<sup>[1]</sup>。若能提高动脉粥样硬化的早期检出率,促使高危人群及早干预,可以推迟甚至避免心血管疾病的发生和发展。

目前,检查血脂、血糖、血半胱氨酸等血液指标可发现致病危险因素<sup>[2]</sup>,但是这些指标需要通过抽血化验得到,为有创检测。现有的超声检查可以检测到颈动脉、下肢动脉等动脉病变<sup>[3-4]</sup>;X 射线检测可以发现主动脉粥样硬化所致的血管影增宽和钙化等情况<sup>[5]</sup>;光声成像技术可以根据斑块成分对光的吸收差异来检测和区分动脉粥样硬化斑块,有助于

收稿日期: 2020-08-19; 修回日期: 2020-09-01; 录用日期: 2020-09-15

基金项目: 中国科学院科技服务网络计划 (KFJ-STS-QYZD-184, KFF-STS-ZDTP-063)、安徽省科技重大专项 (201903a07020027, 17030901017, 17030801007)、中国科学院国际合作局对外合作重点项目 (116134KYSB20170018)、安徽省自然科学基金 (1908085QH365)、安徽省重点研发项目 (202004a07020016, 1804b06020350, 1804h08020291)

\*E-mail: dongmeili@aoifm.ac.cn

人们全面了解斑块的形态和成分<sup>[6-7]</sup>;各种血管造影手段可以判断心脏冠状动脉和脑动脉管腔是否狭窄,也可以判断动脉瘤样病变所在的位置、范围以及病变的程度<sup>[8-9]</sup>。以上所有的超声、射线、光声成像技术和造影检查均是在动脉已经出现病变后才能发现异常,在早期检测方面有一定的局限性,且仪器体积较大,不适合用于动脉粥样硬化疾病的大范围早期筛查。

皮肤是胆固醇新陈代谢的重要场所,人体大约有11%的胆固醇存在于皮肤中<sup>[10]</sup>。皮肤中的胆固醇与动脉壁沉积的胆固醇密切相关:随着动脉硬化程度增加,表皮层中胆固醇的含量也会增加<sup>[11]</sup>。多年的研究结果显示,皮肤胆固醇可以作为动脉粥样硬化的新型标志物。高水平皮肤胆固醇沉积是动脉粥样硬化的早期预警信号,可以用于心血管疾病的风险预测<sup>[12-14]</sup>。

常规的皮肤胆固醇测定主要是通过皮肤活检实现的。该方法在获取皮肤样品时会造成受检者疼痛,活检部位有感染的风险,而且活检样品中包含了不同来源的胆固醇,很难得出可靠的胆固醇分析结果。通过胶带剥离法获得皮肤表面胆固醇<sup>[15]</sup>来测定皮肤胆固醇含量的方法,存在检测程序复杂、耗时较长、重复性差、不能及时出结果等缺点。针对皮肤胆固醇检测方法的不足,Lopukin课题组提出了“三滴法”,即:将三种特定浓度且能够与皮肤胆固醇特异性结合的试剂滴加于受检者皮肤表面,通过观察皮肤表面试剂颜色的变化来判断受检者患动脉粥样硬化的风险<sup>[16]</sup>。该测试方法无需空腹,无需抽血或针刺,几分钟内即可获得检测结果。在“三滴法”的基础上,国内研究者提出了基于漫发射光谱法以及

吸收光谱法的皮肤胆固醇检测技术<sup>[17-19]</sup>,这些技术都是在皮肤表面检测反应后试剂的漫反射光谱信息和吸收光谱信息来推算皮肤胆固醇浓度的。然而,“三滴法”也有其局限性:1)容易受到操作者操作习惯的影响;2)检测试剂成分复杂,质控困难,而且检测试剂包含生物大分子(酶)、聚合物和小分子,易受温度、pH等环境因素的影响,长时间保存比较困难;3)“三滴法”检测时需要用到显色剂,对于显色时间需要严格控制,否则测量结果会差别很大。这些局限性限制了“三滴法”的广泛应用。

针对上述方法的不足,本文提出了基于荧光光谱法的皮肤胆固醇无创检测技术。该技术通过测量荧光标记的皮肤荧光光谱信息来反演测量部位皮肤胆固醇含量,从而实现皮肤胆固醇的无创快速检测。与“三滴法”相比,本文所提方法校正了温度对检测结果的影响,检测试剂的稳定性强、成本低,实验操作步骤少,能够提高检测结果的重复性和准确性,适用于大规模人群的皮肤胆固醇筛查。

## 2 检测原理与系统设计

### 2.1 检测原理

皮肤胆固醇检测试剂能够与皮肤胆固醇特异性结合,在激发光照射下能够发射荧光<sup>[20]</sup>,而且与皮肤表面结合的检测试剂的量同皮肤中胆固醇的含量呈正相关。通过特定波长的激发光激发与皮肤胆固醇结合的检测试剂,并测量其荧光发射光谱,就可以反演得到皮肤胆固醇的含量信息。

### 2.2 检测实验系统

根据上述检测原理,本研究团队设计了一种基于荧光光谱法的皮肤胆固醇检测系统,如图1所示。

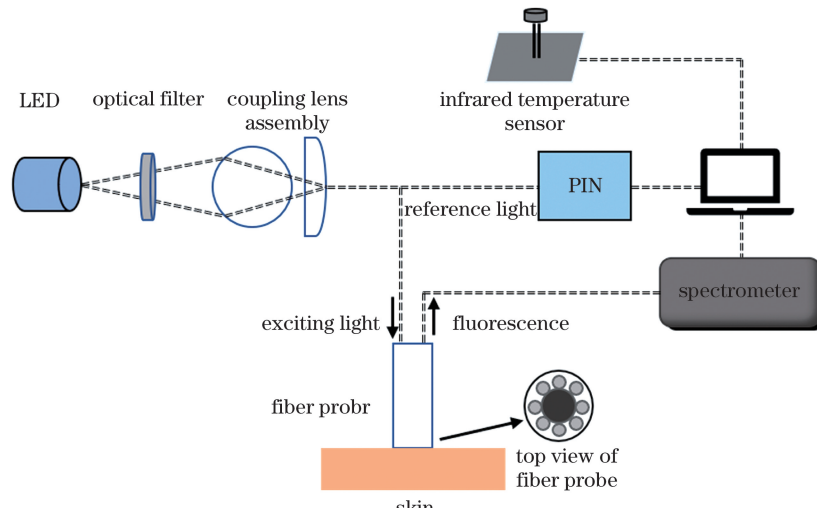


图1 荧光光谱测量系统框图

Fig. 1 Block diagram of fluorescence spectrum measurement system

该检测系统选用中心波长为 430 nm 的 LED 作为激发光源,激发光源发出的光经滤光、耦合透镜组耦合进入石英光纤束,光纤分束器将入射光分为两路:一路作为参考光信号通过光纤到达光电二极管;另一路通过光纤传输至光纤探头,作为激发光激发被检测的皮肤,受激发射荧光被光纤探头收集后经光纤传输至光谱仪,与参考光一起输入到计算机中。鉴于荧光基团荧光效率受温度的影响较大,在检测荧光的同时,通过红外测温传感器收集受试者手掌的温度信息,进而对由温度差异引起的测量误差进行修正。LED 的线宽为 12 nm。本实验使用的是微型光栅光谱仪,其检测波长范围为 200~850 nm,分辨率为 5 nm。光纤纤芯的直径为 0.6 mm,数值孔径为 0.22,入射光纤与收集光纤近边缘距离为 0.4 mm。红外测温传感器采用的是 MLX90615。

在检测过程中,由于测量的荧光光谱中携带了

皮肤的背景荧光,因此在计算胆固醇浓度时,首先从测量得到的荧光光谱中扣除皮肤背景,再将修正后的荧光光谱与荧光标准光谱进行最小二乘拟合,然后进行温度和光源强度的修正,即可得到皮肤胆固醇的含量信息。根据检测试剂的荧光光谱特征,本文选择 400~600 nm 作为特征波段进行分析处理。

### 2.3 检测流程

皮肤胆固醇检测流程如图 2 所示。首先用酒精棉擦拭手掌小鱼际,对待测部位进行清洁;将涂覆板贴合于皮肤表面,确保检测试剂在滴加至皮肤表面时不会外漏;将手掌放置于检测系统的测量孔上,测量皮肤的背景光谱;滴加检测试剂至涂覆板检测孔内;待检测试剂与皮肤胆固醇结合 1 min 后,用吸水棒吸出多余未反应的试剂;再滴加清洗试剂至检测孔清洗 30 s;清洗完成后用吸水棒吸出清洗试剂;最后将待测部位对准检测系统的测量孔,进行测量。单次进行皮肤胆固醇检测实验的总时间在 4 min 以内。



图 2 检测流程图

Fig. 2 Diagram of detection flow

## 3 实验结果及分析

### 3.1 温度对检测试剂荧光效率的影响

温度会直接影响荧光基团的荧光效率。不同人的手掌温度存在差异性,同一人的手掌温度也会随着外界环境温度的变化而变化,因此,手掌温度的差异性会导致检测结果不准确。本系统引入了温度探

测模块,该模块可实时获得受试者手掌的温度信息,从而可以对温度差异引起的测量误差进行修正。

为了进一步研究温度对荧光基团荧光效率的影响,同时也为了给测量误差的修正提供参考,本文对检测试剂的荧光温度特性进行了测量,测量装置如图 3 所示。光源输出的光被光纤一分为二,一路直接由光谱仪 I 接收,用以监测光源强度的变化情况;

另一路作为激发光直接照射荧光检测试剂,检测试剂的荧光发射光谱由光谱仪Ⅱ接收。其中,检测试剂放置在一个比色皿中,比色皿放置于TEMI880系列可程式恒温恒湿实验箱中。

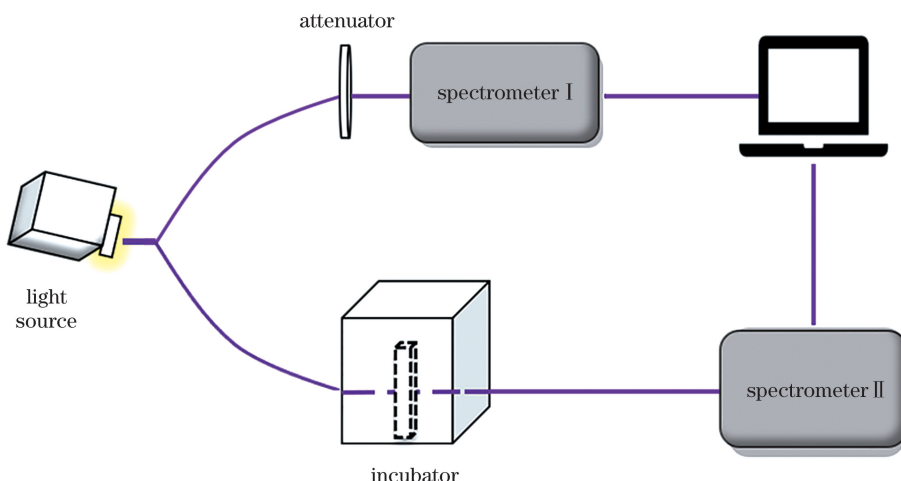


图3 检测试剂响应曲线的实验装置图

Fig. 3 Test equipment diagram of detection reagent response curve

环境温度不同,人体皮肤温度会明显不同。在稳态均匀的冷环境( $15.6^{\circ}\text{C}$ )、中性环境和暖环境( $31.5^{\circ}\text{C}$ )下,手部皮肤温度的变化范围是 $21.1\sim36.4^{\circ}\text{C}$ <sup>[21]</sup>。因此,实验时将恒温恒湿实验箱的温度分别设定为 $20, 24, 28, 32, 36, 40^{\circ}\text{C}$ ,相对湿度设为50%。待温度稳定后,分别记录光源光谱和荧光发射光谱,每组数据重复测量三次。结果表明,在测

量过程中,光源光强的波动在 $\pm 0.4\%$ 以内。

不同温度下检测试剂的原始荧光光谱如图4(a)所示。从图4(a)中可以看出,随着温度升高,检测试剂的荧光发射光谱形状保持不变,强度逐渐减弱。图4(b)为扣除暗背景以及采用Savitzky-Golay平滑法处理后的荧光光谱,光谱曲线整体平滑,保留了相应的波峰,无毛刺等噪声。

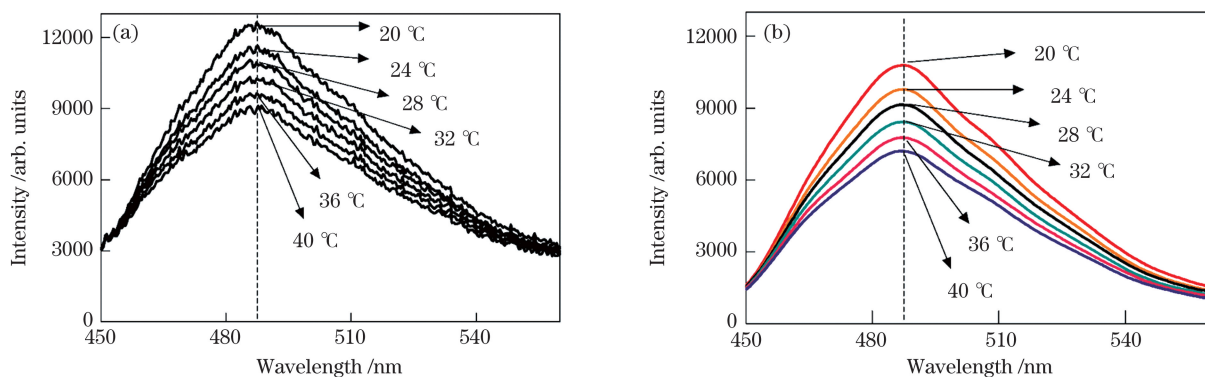


图4 不同温度下检测试剂的荧光光谱。(a)原始荧光光谱图;(b)经过平滑处理后的荧光光谱图

Fig. 4 Fluorescence spectra of detection reagent at different temperatures. (a) Original fluorescence spectra; (b) fluorescence spectra after smoothing

在进行光谱分析处理时,有一部分光谱区域不含有效信息或容易受其他因素的影响,若将整体光谱代入分析会影响计算结果的准确性。因此,本文根据得到的光谱曲线特征,选择特征单波长或波段,利用该波长或波段的相关信息进行分析。

由荧光光谱曲线可知,在 $487\text{ nm}$ 处检测试剂的荧光强度达到了最高值,本文将这个峰值波长作为特征单波长。根据荧光光谱曲线的特征, $20^{\circ}\text{C}$ 时

测量的荧光光谱的半峰全宽对应波段( $462\sim520\text{ nm}$ )内的曲线易于区分,因此选用该波段作为特征波段。以温度作为横坐标,检测试剂的荧光强度作为纵坐标作图,如图5所示。可以看出:在特征波长处和特征波段范围内,随着温度升高,检测试剂的荧光强度均呈线性减小,经最小二乘拟合后的判定系数分别为 $R^2=0.992$ ( $487\text{ nm}$ 处)和 $R^2=0.990$ ( $462\sim520\text{ nm}$ 波段内);检测试剂的

荧光强度与温度呈显著负相关,相关系数 $r$ 分别为 $-0.996$ 和 $-0.995$ 。结果表明:在手掌温度变化范围内,无论是在特征单波长487 nm处,还是在特征波段462~520 nm内,检测试剂的荧光强度均随温度线性变化;但单波长点存在波动较大

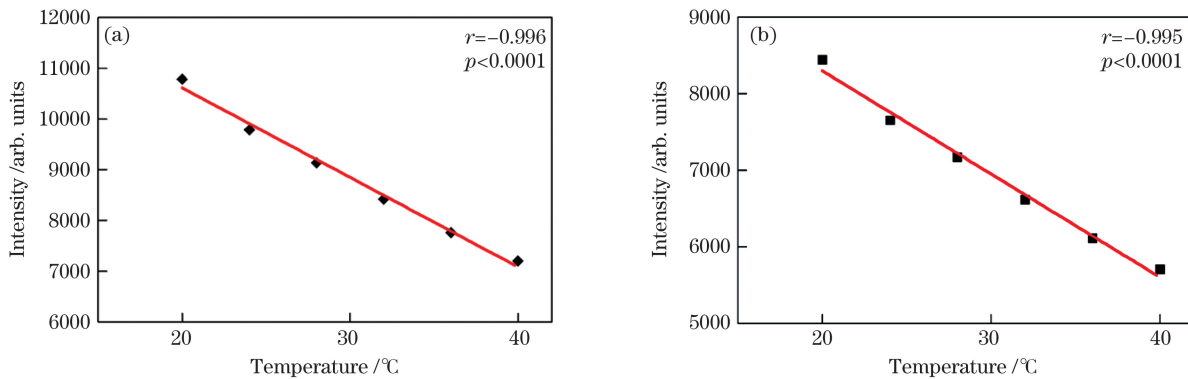


图5 检测试剂荧光强度随温度的变化。(a)在特征单波长487 nm处;(b)在特征波段462~520 nm内

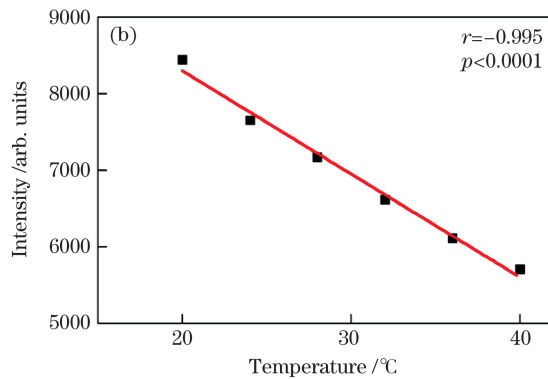
Fig. 5 Variation of fluorescence intensity of detection reagent changes with temperature. (a) At characteristic wavelength 487 nm; (b) in characteristic wavelength band of 462–520 nm

### 3.2 系统准确性的验证

为了验证本系统在皮肤胆固醇检测方面的准确性,本文将系统测量结果与气相色谱测量结果进行了比对。胆固醇萃取液可以萃取出部分皮肤角质层中的胆固醇,皮肤中的胆固醇含量越高,萃取液中的胆固醇含量就越高<sup>[22]</sup>。

本研究团队征集了80名受试者进行准确性验证实验,本次实验通过了中国科学院合肥物质科学研究院医学伦理委员会的伦理审批。实验中,先用本文的检测系统检测受试者皮肤胆固醇含量;检测完成后,用400 μL无水乙醇提取检测部位皮肤胆固醇2 min,得到皮肤胆固醇萃取液,然后将胆固醇标准溶液溶于无水乙醇中(胆固醇的质量浓度分别为1,2,5,10,25,50 μg/mL),采用气相色谱法检测胆固醇含量<sup>[23]</sup>。检测条件如下:色谱柱,DB-5弹性石英毛细管柱;载气选择高纯氮气,纯度≥99.99%,恒定流量(2.4 mL/min);柱温(程序升温)的初始温度为200 °C,保持1 min,然后以30 °C/min的升温速率升至280 °C,保持10 min;进口温度为280 °C;检测器温度为290 °C;进样量为1 μL;进样方式为不分裂注射,注射1 min后打开阀门;空气流量为350 mL/min;氢气流量为30 mL/min。将胆固醇标准溶液分别注入气相色谱仪中,在上述色谱条件下测定标准溶液的峰面积,然后以质量浓度为横坐标,峰面积为纵坐标,绘制标准曲线。然后将皮肤胆固醇萃取液注入气相色谱仪中测定峰面积,通过标

的风险,会对结果的重复性和准确性产生影响,而在特征波段462~520 nm内,采用平均荧光强度能够弥补这种不足。在皮肤胆固醇测量过程中,可通过校准曲线对温度差异性进行修正,提高测量的准确性和稳定性。



准曲线得到样品溶液中胆固醇的浓度。

接下来分析系统测量值与气相色谱法测量值之间的相关性。如图6所示,采用荧光光谱法测得的皮肤胆固醇含量与气相色谱法测量值之间显著相关, $r=0.905$ ( $p<0.0001$ ),验证了该系统在皮肤胆固醇含量测量方面的可行性。

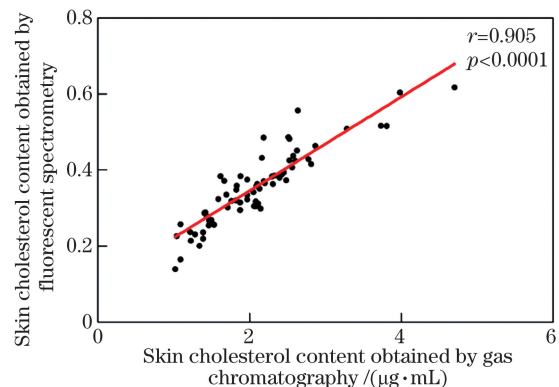


图6 气相色谱法与荧光光谱法的相关性分析

Fig. 6 Correlation analysis between gas chromatography and fluorescent spectrometry

### 3.3 皮肤胆固醇无创检测临床验证

为了进一步验证该系统的临床应用价值,分别对正常人群和动脉粥样硬化高风险人群的皮肤胆固醇含量进行检测。

本次临床验证招募了89名受试者,其中男性39名,女性50名,受试者均无传染性皮肤疾病,被测量手掌的小鱼际部位皮肤完整、无疤痕、无苔藓样

硬化斑或畸形,无严重心、肺、肾功能不全,近一个月内未服用任何降脂类药物。本次实验通过了安徽省立医院医学研究伦理委员会的伦理审批。在室温条件下,根据图2所示的检测流程,对受试者手掌小鱼际处皮肤胆固醇含量进行检测,并收集受试者血脂及颈动脉内膜中层厚度(CIMT)信息。综合临床信息和皮肤胆固醇测量值,用SPSS 24.0软件对数据进行分析处理。

CIMT是影响动脉粥样硬化性疾病的重要因素之一<sup>[24-25]</sup>,CIMT的增厚与动脉粥样硬化严重程度显著相关,可以作为动脉粥样硬化诊断的依据<sup>[26]</sup>。根据CIMT指标,将受试人群分为正常组和高风险组,CIMT小于1.0 mm的人群为正常组,CIMT不小于1.0 mm的人群为高风险组。分组后,正常组43人,高风险组46人。不同人群皮肤胆固醇的检测结果如图7所示,可见,正常组皮肤胆固醇含量均值为0.36,高风险组皮肤胆固醇含量均值为0.42。

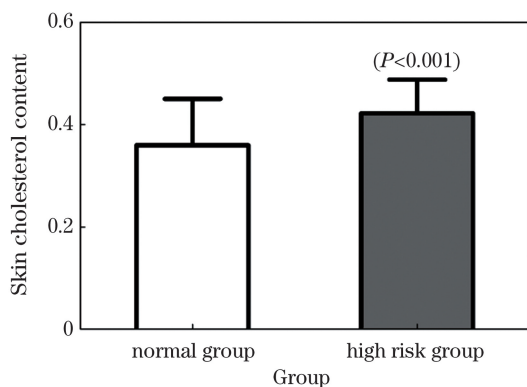


图7 正常组和动脉粥样硬化高风险组的检测结果

Fig. 7 Skin cholesterol contents of normal and atherosclerosis high risk groups

采用t检验法对两组数据进行分析,两组人群皮肤胆固醇含量有显著性差异, $P < 0.001$ ( $P = 0.0004$ )。这表明,该无创检测系统可以用于动脉粥样硬化高风险人群的筛查。

## 4 结 论

本研究团队基于荧光光谱法设计了一种皮肤胆固醇快速无创检测系统。该系统通过测量与皮肤胆固醇特异性结合的检测试剂的荧光光谱,快速反演出了测量部位皮肤胆固醇含量。该系统设计有温度和光源强度修正模块,能够对温度和光源强度波动引起的测量结果偏差进行修正,提高了系统测量的准确性和稳定性。

本研究团队通过气相色谱法测量了萃取液中的

皮肤胆固醇含量,并将测量结果与系统检测的皮肤胆固醇值进行相关性分析,验证了检测方法的可行性和检测系统的准确性。此外,还采用该系统对动脉粥样硬化高风险人群和正常人群的皮肤胆固醇含量进行了检测,初步结果表明,该系统可应用于动脉粥样硬化高风险人群的筛查。

在接下来的研究中,本团队将招募更多受试者,并综合分析年龄、身高、体重、血脂等相关信息,开展随访研究,确定动脉粥样硬化高风险人群的筛查切点值。该技术具有无创、快速、灵敏度高等优点,适合用于大规模的早期风险筛查。该技术的推广应用对于心血管疾病的防控具有重要意义。

## 参 考 文 献

- [1] Gao P, He Z Y. Clinical analysis of correlation between ankle-brachial index, carotid atherosclerosis and ischemic cerebral infarction [J]. Medical Innovation of China, 2010, 7(36): 98-100.
- 高鹏, 何志义. 踝臂指数、颈动脉粥样硬化与缺血性脑梗死相关性的临床分析[J]. 中国医学创新, 2010, 7(36): 98-100.
- [2] Jiang H, Cao L S. Diagnosis and treatment of dyslipidemia [J]. Journal of Clinical Cardiology, 2004, 20(10): 638-640.
- 姜红, 曹林生. 血脂异常的诊断与治疗[J]. 临床心血管病杂志, 2004, 20(10): 638-640.
- [3] Veronese E, Tarroni G, Visentini S, et al. Estimation of prenatal aorta intima-media thickness from ultrasound examination[J]. Physics in Medicine and Biology, 2014, 59(21): 6355-6371.
- [4] Li J K, Chen X D, Wang Y, et al. Sidelobe canceller algorithm for ultrasonic imaging [J]. Laser & Optoelectronics Progress, 2019, 56(7): 071103.
- 李嘉科, 陈晓冬, 汪毅, 等. 适用于超声成像的旁瓣相消算法[J]. 激光与光电子学进展, 2019, 56(7): 071103.
- [5] Basu S P, Sen Gupta B K. Radiographic study of the heart and the aorta in atherosclerosis [J]. Bulletin of the Calcutta School of Tropical Medicine, 1966, 14(3): 90-91.
- [6] Liu Q, Jin T, Chen Q, et al. Research progress of miniaturized photoacoustic imaging technology in biomedical field[J]. Chinese Journal of Lasers, 2020, 47(2): 0207019.
- 刘强, 金天, 陈倩, 等. 小型化光声成像技术在生物医学领域的研究进展[J]. 中国激光, 2020, 47(2): 0207019.
- [7] Long X Y, Tian C. Biomedical photoacoustic microscopy: advances in technology and applications

- [J]. Chinese Journal of Lasers, 2020, 47(2): 0207016.  
龙晓云, 田超. 生物医学光声显微成像: 技术和应用进展[J]. 中国激光, 2020, 47(2): 0207016.
- [8] Girardet M, Jacotot B, Cachera J P, et al. Cutaneous cholesterol in coronary disease in man. Comparison of 2 technics of extraction[J]. Paroi Arterielle, 1977, 4(1): 59-63.
- [9] Zhang F, Chen X T, Zhang X H. Algorithm of automatic detection of blood vessel stenosis with sub-pixel level of digital subtraction angiography [J]. Laser & Optoelectronics Progress, 2018, 55(4): 041101.  
张帆, 陈相廷, 张新红. 数字减影血管造影的影像血管狭窄亚像素级自动检测算法[J]. 激光与光电子学进展, 2018, 55(4): 041101.
- [10] Mazzone T, Pustelnikas L. Growth-related modulation of human skin fibroblast cholesterol distribution and metabolism [J]. Biochimica et Biophysica Acta (BBA)-Lipids and Lipid Metabolism, 1990, 1047(2): 180-186.
- [11] Bouissou H, de Graeve J, Legendre C, et al. Skin cholesterol and skin apoprotein B in atherosclerosis [J]. Biomedicine & Pharmacotherapy, 1982, 36(3): 159-162.
- [12] Melico-Silvestre A A, Jacotot B, Buxtorf J C, et al. Study of free and esterified cholesterol in skin in atherogenic hyperlipidemias [J]. Pathologie-biologie, 1981, 29(9): 573-578.
- [13] Sprecher D L, Goodman S G, Kannampuzha P, et al. Skin tissue cholesterol (SkinTc) is related to angiographically-defined cardiovascular disease [J]. Atherosclerosis, 2003, 171(2): 255-258.
- [14] Tashakkor A Y, Mancini G B J. The relationship between skin cholesterol testing and parameters of cardiovascular risk: a systematic review[J]. Canadian Journal of Cardiology, 2013, 29(11): 1477-1487.
- [15] Lademann J, Jacobi U, Surber C, et al. The tape stripping procedure - evaluation of some critical parameters [J]. European Journal of Pharmaceutics and Biopharmaceutics, 2009, 72(2): 317-323.
- [16] Zawydiwski R, Sprecher D L, Evelegh M J, et al. A novel test for the measurement of skin cholesterol [J]. Clinical Chemistry, 2001, 47(7): 1302-1304.
- [17] Hou H Y, Fang Z H, Zhang Y Z, et al. Simulation and *in vivo* experimental study on noninvasive spectral detection of skin cholesterol [J]. Chinese Journal of Lasers, 2016, 43(9): 0907001.  
候华毅, 方朝晖, 张元志, 等. 皮肤胆固醇无创光谱检测模拟和在体实验研究[J]. 中国激光, 2016, 43(9): 0907001.
- [18] Hou H Y, Dong M L, Wang Y K, et al. Rapid and noninvasive detection of skin cholesterol with diffuse reflectance spectroscopy technology [J]. Spectroscopy and Spectral Analysis, 2016, 36(10): 3215-3221.  
候华毅, 董美丽, 王贻坤, 等. 漫反射光谱技术快速无创检测皮肤胆固醇[J]. 光谱学与光谱分析, 2016, 36(10): 3215-3221.
- [19] Xu C, Fang Z H, Dong M L, et al. Design of non-invasive skin cholesterol detection system based on absorption spectroscopy [J]. Opto-Electronic Engineering, 2018, 45(4): 24-31.  
许超, 方朝晖, 董美丽, 等. 基于吸收光谱技术的皮肤胆固醇无创检测系统设计[J]. 光电工程, 2018, 45(4): 24-31.
- [20] Liu Y, Wang Y K, Ni J S, et al. Fluorescence detecting reagent and its preparation method, and system and method for measuring skin cholesterol: CN108204963A[P]. 2018-06-26.  
刘勇, 王贻坤, 倪敬书, 等. 一种荧光检测试剂及制备方法及用于皮肤胆固醇的测量系统及方法: CN108204963A[P]. 2018-06-26.
- [21] Huizenga C, Zhang H, Arens E, et al. Skin and core temperature response to partial- and whole-body heating and cooling [J]. Journal of Thermal Biology, 2004, 29(7/8): 549-558.
- [22] Dinh T T N, Thompson L D, Galyean M L, et al. Cholesterol content and methods for cholesterol determination in meat and poultry [J]. Comprehensive Reviews in Food Science and Food Safety, 2011, 10(5): 269-289.
- [23] Torkhovskaya T I, Fortinskaya E S, Khalilov É M, et al. Quantity of cholesterol extracted from the human skin surface: a possible discriminant of atherosclerosis? [J]. Bulletin of Experimental Biology and Medicine, 1992, 113(5): 645-648.
- [24] Stein J H, Tzou W S, DeCara J M, et al. Usefulness of increased skin cholesterol to identify individuals at increased cardiovascular risk (from the predictor of advanced subclinical atherosclerosis study) [J]. The American Journal of Cardiology, 2008, 101(7): 986-991.
- [25] Tzou W S, Mays M E, Korcarz C E, et al. Skin cholesterol content identifies increased carotid intima-media thickness in asymptomatic adults [J]. American Heart Journal, 2005, 150(6): 1135-1139.
- [26] Grobbee D E, Bots M L. Carotid artery intima-media thickness as an indicator of generalized atherosclerosis [J]. Journal of Internal Medicine, 1994, 236(5): 567-573.

## Rapid Non-Invasive Technology for Skin Cholesterol Detection Based on Fluorescent Spectrometry

Wu Peng<sup>1,2</sup>, Ni Jingshu<sup>2,4</sup>, Hong Haiou<sup>3</sup>, Li Xiaojing<sup>3</sup>, Yao Bei<sup>3</sup>, Zheng Haoran<sup>3</sup>, Hua Changyi<sup>2,4</sup>, Wang Xia<sup>2,4</sup>, Zhang Yuanzhi<sup>2,4</sup>, Zhang Yang<sup>2,4</sup>, Wang Yikun<sup>2,4</sup>, Dong Meili<sup>2,4\*</sup>

<sup>1</sup> College of Physics and Electronic Information, Anhui Normal University, Wuhu, Anhui 241000, China;

<sup>2</sup> Anhui Provincial Engineering Laboratory for Medical Optical Diagnosis & Treatment Technology and Instrument, Anhui Institute of Optics and Fine Mechanics, Hefei Institute of Physical Science, Chinese Academy of Sciences, Hefei, Anhui 230026, China;

<sup>3</sup> Health Management Centre, the First Affiliated Hospital of University of Science and Technology of China, Hefei, Anhui 230001, China;

<sup>4</sup> Anhui Provincial Engineering Technology Research Center for Biomedical Optical Instrument, Wanjiang Center for Development of Emerging Industrial Technology, Tongling, Anhui 244000, China

### Abstract

**Objective** Skin cholesterol is an important biomarker for early atherosclerosis screening. Atherosclerosis is the leading cause of disability and death from cardiovascular disease. Effective control of pathogenic factors in the early pathological stage may delay or prevent the development of asymptomatic atherosclerosis into cardiovascular diseases. Thus, skin cholesterol detection becomes relevant in the prevention of cardiovascular diseases. Traditional skin cholesterol detection methods, such as skin biopsy or tape stripping, are invasive and usually time consuming. Alternatively, the recent three-drop method is being widely studied. In this method, three specific concentrations of reagents that bind to skin cholesterol are used on the skin surface of a subject, and atherosclerosis can be diagnosed by analyzing the reagent color changes. However, the three-drop method is sensitive to the application habits of the operator. Moreover, the detection reagents contain enzymes, polymers, and small molecule compounds, hindering quality control and increasing the sensitivity to environmental factors such as temperature and pH levels. We report a non-invasive skin cholesterol detection technique based on fluorescent spectrometry. By measuring the fluorescence spectrum of fluorescent-labeled skin, the cholesterol content can be calculated from the fluorescence spectra. This method corrects the influence of temperature on the test results and provides stability under various environmental conditions. Moreover, the skin cholesterol content can be obtained within 4 minutes. The proposed method provides a rapid non-invasive and stable method for skin cholesterol detection and corresponding applications including early atherosclerosis screening.

**Methods** The proposed non-invasive skin cholesterol detection system is composed of a light source, fiber probe, spectrometer, photodiode, infrared temperature sensor, and computer. The fluorescence fluctuation of the detection reagent caused by temperature variation is corrected by establishing the relation between temperature and the fluorescence intensity of the detection reagent. To confirm the accuracy of the proposed skin cholesterol detection system, we extract skin cholesterol with absolute ethanol after the non-invasive measurement. The cholesterol content in the extraction liquid is determined by gas chromatography, and the correlation between the two results are analyzed. Finally, the clinical applicability of the proposed system is confirmed by measuring skin cholesterol content from both healthy subjects and subjects with high risk of presenting atherosclerosis.

**Results and Discussions** The schematic of the proposed non-invasive skin cholesterol detection system based on fluorescent spectrometry is shown in Fig. 1. The system accurately detects skin cholesterol content after correcting for temperature. The average fluorescence intensity of the detection reagent in the 462–520 nm wavelength band decreases with increasing temperature, resulting in a significant negative correlation between fluorescence intensity and temperature ( $r = -0.995$ ,  $p < 0.0001$ ). This relation can be used to establish a calibration curve to correct for temperature (Fig. 5). We recruited 80 subjects to verify the accuracy of the proposed system. The skin cholesterol content measured using the proposed temperature-corrected system is highly correlated (correlation coefficient of 0.905) with that measured using gas chromatography (Fig. 6). These results verify the accuracy of the proposed

system to measure skin cholesterol. To verify whether the proposed system can distinguish healthy subjects from subjects with high risk of presenting atherosclerosis, we used the system in 43 and 46 subjects from the respective groups. There is a significant difference in skin cholesterol content between the healthy and high risk samples ( $p = 0.0004$ ) (Fig. 7). The proposed non-invasive skin cholesterol detection system can screen subjects with high risk of presenting atherosclerosis. Nevertheless, clinical trials are required for verification given the small sample size used in this study.

**Conclusions** We propose a rapid non-invasive detection system for skin cholesterol based on fluorescent spectrometry. The system quickly provides the skin cholesterol content on-site from the fluorescence spectrum of detection reagents that specifically bind to skin cholesterol. The proposed system performs temperature correction to prevent deviations of the measurement results and improve accuracy and stability. The system and its detection accuracy are verified through comparisons with skin cholesterol results obtained from gas chromatography. The proposed system may be used to screen people with high risk of presenting atherosclerosis by detecting skin cholesterol content in healthy subjects and subjects at high risk. Overall, the proposed system can detect skin cholesterol accurately, non-invasively, and quickly. We expect that the widespread adoption of this technology will contribute to the prevention and control of cardiovascular diseases.

**Key words** medical optics; skin cholesterol; fluorescent spectrometry; non-invasive detection; atherosclerosis

**OCIS codes** 170.4580; 170.3890; 170.6280; 170.6930